Tracking control for a flat system under disturbances: a fixed-wing UAV example

Huu Thinh Do, Florentina Nicolau, Florin Stoican, Ionela Prodan

Tracking control for a flat system under disturbances: a fixed-wing UAV example

Huu Thinh Do * **Florentina Nicolau** ** **Florin Stoican** *** **Ionela Prodan** *

* *Univ. Grenoble Alpes, Grenoble INP*†*, LCIS, F-26000, Valence, France, (e-mail: {huu-thinh.do,ionela.prodan}@lcis.grenoble-inp.fr).*
† *Institute of Engineering and Management Univ. Grenoble Alpes.*
** *Quartz EA 7393, ENSEA, 95014 Cergy-Pontoise Cedex and Université Paris-Saclay, CNRS, CentraleSupélec, Laboratoire des signaux et systèmes, 91190, Gif-sur-Yvette, France. (e-mail: florentina.nicolau@ensea.fr)*
*** *Politehnica University of Bucharest, ACSE, Bucharest, Romania, (e-mail: florin.stoican@upb.ro)*

Abstract: This paper considers a class of systems admitting several flat representations and proposes a trajectory tracking controller design which accounts for disturbance rejection. Set invariance is used for characterizing the tracking and estimation error dynamics. Furthermore, some insights on the disturbance propagation in case of different flat representations for a fixed-wing Unmanned Aerial Vehicle (UAV) system are highlighted via simulations and comparisons.

Keywords: Trajectory tracking, Unmanned Aerial Vehicle, Differential flatness, Disturbance rejection, Extended state observer, Set invariance.

1. INTRODUCTION

Introduced in the 1990s, the definition of differentially flat systems (Fliess et al., 1993) has drawn a significant amount of attention thanks to the guaranteed explicit representation of nonlinear systems simply via the evolution of an $m-$tuple of functions (where m is the number of control inputs), called *flat output,* i.e, the evolution in time of all state and control variables can be recovered from that of the flat output and a finite number of its time-derivatives. This property benefits not only the *trajectory generation problem*, but also the *control design procedure.* More specifically, thanks to this representation, the system's planning problem is reduced to the planning of the flat output and so are the ancillary requirements such as input saturation (Nguyen et al., 2020), obstacle avoidance (Stoican et al., 2015b) or minimization of energy spent (Zafeiratou et al., 2020). Furthermore, after achieving a feasible reference trajectory which directly takes into account the system's dynamics and constraints, one can also exploit flatness to simplify the feedback control design process. A linearization law can be proposed to cancel out the nonlinearities via dynamic, invertible and endogenous feedback transformations that convert the system into a linear equivalent controllable dynamics. The remaining problem is to control the linear dynamics properly. Several methods have been exploited since this type of transformation was introduced, including state feedback, sliding mode control or backstepping-based control (Sira-Ramírez, 2015; Martin, 1994).

When addressing the flatness-based control design and analysis, seldom are the proposed solutions combined with the *set theoretic framework* in order to evaluate the robustness and efficiency of the system's performance. Furthermore, although the flat output is a function of the state, input and its derivatives, it is well known that the representation is not unique (Kaminski et al., 2018). Hence, an interesting question arises: *among a set of flat outputs, which is better suited for control synthesis from the viewpoint of disturbance rejection performance?*

The main goal of this paper is to provide a reliable tracking controller design based on flatness and its properties while evaluating the influence of the disturbance propagation when considering different flat output representations. Our contributions can be briefly summarized as follows:

- we provide a systematic procedure for controller and observer design for a class of systems which admit a flat output representation affected by disturbances;
- we analyse the effect of changing the flat output selection on the controller construction and the performance from a set-theoretic viewpoint;
- we provide numerical simulation and discussions for a particular flat system i.e., a fixed-wing UAV model.

The remainder of the paper is organized as follow: Section 2 summarizes the entire procedure including the transformation of the nonlinear system into a linear equivalent one, controller and observer design, and set descriptions for performance assessment. Section 3 applies the proposed framework for a 3 degree of freedom (3-DOF) UAV model under disturbances. Numerical simulations and discussions are provided in Section 4. Finally, Section 5 draws the conclusions and indicates some future directions of research.

⋆ This work is supported by the French National Research Agency in the framework of the "Investissements d'avenir " program "ANR-15-IDEX-02" and the LabEx PERSYVAL "ANR-11-LABX-0025-01". It is also partially supported by a grant of the Romanian Ministry of Education and Research, CNCS - UEFISCDI, project number PN-III-P1-1.1-TE-2019-1614, within PNCDI III.

2. PREREQUISITES

In this section, the notion of flatness will be recalled to construct a foundation for the subsequence feedback linearization design process. The linearized dynamics will be then taken into account together with bounded disturbances via the construction of an extended state observer (ESO). Finally, as an approach to evaluate the efficiency of the method, *robust positive invariant sets* of the linearized tracking and estimation error dynamics will be computed and analysed. Let us first introduce the notations and mathematical tools exploited throughout the paper.

Notation: Denote by upper-case letters the matrices with appropriate dimension. Let also $\boldsymbol{I}_n$ represent the identity matrix of dimension $(n \times n)$ while $\mathbf{0}_{(a\times b)}$ denotes the null matrix of size $(a \times b)$ and $\mathbf{1}$ is the matrix of ones with suitable size. Vectors will be denoted in bold (e.g. $\boldsymbol{\xi}$, $\boldsymbol{u}$).

2.1 Model inversion through flatness

We consider the following nonlinear control system under the presence of disturbances as in (1):

$$\dot{\boldsymbol{\xi}} = f(\boldsymbol{\xi}, \boldsymbol{u}) + \boldsymbol{d}_\xi, \tag{1}$$

where $\boldsymbol{\xi}, \boldsymbol{d}_\xi \in \mathbb{R}^n$ and $\boldsymbol{u} \in \mathbb{R}^m$ are respectively the system's state, disturbance and input vector. We suppose that the nominal model $\dot{\boldsymbol{\xi}} = f(\boldsymbol{\xi}, \boldsymbol{u})$ is flat, that is, there exists a m-dimensional smooth vector valued function $\varphi\left(\boldsymbol{\xi}, \boldsymbol{u}, \dot{\boldsymbol{u}}, ..., \boldsymbol{u}^{(p)}\right)$ for some integer $p \geq 0$, such that both the state and the input can be expressed in terms of $\boldsymbol{z} = \varphi(\boldsymbol{\xi}, \boldsymbol{u}, \dot{\boldsymbol{u}}, \ddot{\boldsymbol{u}}, ..., \boldsymbol{u}^{(p)})$, that is called flat output, and a finite number of its time-derivatives:

$$\boldsymbol{\xi} = \Phi_\xi(\boldsymbol{z}, \dot{\boldsymbol{z}}, \ddot{\boldsymbol{z}}, ..., \boldsymbol{z}^{(q-1)}), \tag{2a}$$

$$\boldsymbol{u} = \Phi_u(\boldsymbol{z}, \dot{\boldsymbol{z}}, \ddot{\boldsymbol{z}}, ..., \boldsymbol{z}^{(q)}). \tag{2b}$$

As mentioned in (Levine, 2009), all flat systems can be linearized in closed-loop with an invertible endogenous dynamic feedback law. More precisely, system (1) may be linearized via a dynamic feedback defined as:

$$\dot{\boldsymbol{\eta}} = \alpha(\boldsymbol{\xi}, \boldsymbol{\eta}, \boldsymbol{v}), \text{ and } \boldsymbol{u} = \beta(\boldsymbol{\xi}, \boldsymbol{\eta}, \boldsymbol{v}), \tag{3}$$

with $\boldsymbol{\eta} \in \mathbb{R}^h$, $\boldsymbol{v} = [v_1, ..., v_m]^\top \in \mathbb{R}^m$ and $\beta(\cdot)$ is invertible with respect to $\boldsymbol{v}$. The word "endogenous" reflects the fact that the feedback variables $\boldsymbol{\eta}$ and $\boldsymbol{v}$ are generated by the original ones $(\boldsymbol{\xi}, \dot{\boldsymbol{u}}, \ddot{\boldsymbol{u}}, ...)$, Martin (1994), and often the linearizing dynamic feedback corresponds to dynamical extensions of suitably chosen controls (that is, to use control no longer as the original inputs, which become state of the extended system, but their derivatives). From this, it follows that whenever system (1) admits a flat output $\boldsymbol{z}$, then we can transform it, for some r_i, by a feedback of form (3) and coordinate change into the linear controllable dynamics (Levine, 2009):

$$z_i^{(r_i)} = v_i, \quad 1 \leq i \leq m. \tag{4}$$

This system then can be controlled by applying suitable controllers on each row of (4). For trajectory following, the convergence of z_i to its reference will result in the tracking of the state $\boldsymbol{\xi}$ in the light of the mapping (2a). However, this affirmation can only be satisfied with the nominal model, i.e, when no disturbances (including model uncertainties, external perturbations, etc.) are taken into account. Hence, the next subsection will handle the disturbance rejection by constructing an ESO, which provides estimation for both state and disturbances. Then based on that estimation, a state feedback controller is introduced to counteract the effect of disturbances. Generally, the control scheme (illustrated in Fig. 1) is epitomized as:

- Firstly, the trajectory of the flat output vector $\boldsymbol{z}_{ref} = [z_{1\,ref}, z_{2\,ref}, ..., z_{m\,ref}]^\top$ will be generated such that certain constraints will be respected (dynamics, waypoint passing, obstacle avoidance constraints, etc).
- The tracking is then tackled by the controller in the flat output space where the dynamics is linearized in closed-loop. Both tasks are carried out owing to the feedback from an ESO (Yang and Huang, 2009).
- The real input $\boldsymbol{u}$ is then recovered from the virtual input v_i via the flatness-based inversion in (3).
- The flat output z_i then is measured and given as the input for the observer (9) which, in turn, estimates its derivatives and the disturbance d_i affecting $z_i^{(r_i)}$ and propagated from the state disturbance $\boldsymbol{d}_\xi$.

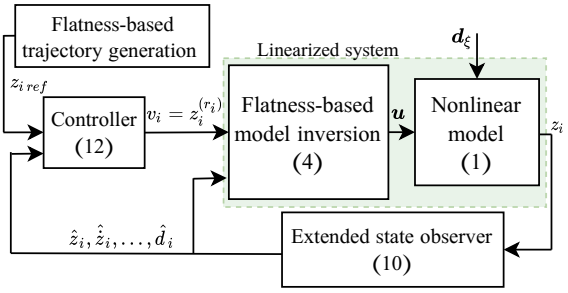

Fig. 1. Flatness-based trajectory tracking control scheme.

Remark 1. Note that the trajectory generation task is an important stage for the entire control scheme as it facilitates the control effort by taking into account beforehand complex problems such as constraint satisfaction or optimal trajectory generation . The trajectory generation using flatness, denoted here and in the figure by $z_{i\,ref}$, can be found in our previous work (Stoican et al., 2015b).

2.2 Tracking controller design with disturbance rejection

Consider the disturbances $\boldsymbol{d}_\xi$ in (1). By applying the same flatness-based linearization law as in (3), the dynamics (1) is transformed into a system of differential equations:

$$z_i^{(r_i)} = v_i + d_i, \tag{5}$$

where d_i is the propagated disturbances through the linearizing procedure. The objective is to ensure that the output z_i tracks its a priori given reference signal $z_{i\,ref}$.

Further, we proceed by rewriting each equation of (5) in a classical state-space representation as follows:

$$\dot{\boldsymbol{\sigma}}_i = A_i\boldsymbol{\sigma}_i + B_i v_i + E_i\tau_i \;\; (1 \leq i \leq m), \tag{6}$$

$$\begin{cases} \boldsymbol{\sigma}_i &= \left[\sigma_{i,1} \;\; \sigma_{i,2} \;\; ... \;\; \sigma_{i,r_i} \;\; \sigma_{i,(r_i+1)}\right]^\top \\ &\triangleq \left[z_i \;\; \dot{z}_i \;\; ... \;\; z_i^{(r_i-1)} \;\; d_i\right]^\top, \\ \tau_i &= \dot{d}_i, \end{cases} \tag{7}$$

$$A_i = \begin{bmatrix} \mathbf{0}_{r_i\times 1} & \boldsymbol{I}_{r_i} \\ 0 & \mathbf{0}_{1\times r_i} \end{bmatrix}, B_i = \begin{bmatrix} \mathbf{0}_{(r_i-1)\times 1} \\ 1 \\ 0 \end{bmatrix}, E_i = \begin{bmatrix} \mathbf{0}_{r_i\times 1} \\ 1 \end{bmatrix}. \tag{8}$$

Considering $y_i = C_i\boldsymbol{\sigma}_i \triangleq [1 \;\; \mathbf{0}_{1\times r_i}]\,\boldsymbol{\sigma}_i$ as the output of (6) and that the pair of matrices (A_i, C_i) is observable, we construct for the linear model (6) an observer as follow:

$$\dot{\hat{\boldsymbol{\sigma}}}_i = A_i\hat{\boldsymbol{\sigma}}_i + B_i v_i + L_i(y_i - \hat{y}_i), \tag{9}$$

where $\hat{\boldsymbol{\sigma}}_i \triangleq [\hat{\sigma}_{i,1} \;\; ... \;\; \hat{\sigma}_{i,(r_i+1)}]^\top$ is the estimated value of $\boldsymbol{\sigma}_i$ and $\hat{y}_i$ is that of y_i. The estimation error between the current and the estimated value $\hat{\boldsymbol{e}}_i = \boldsymbol{\sigma}_i - \hat{\boldsymbol{\sigma}}_i$ yields:

$$\dot{\hat{\boldsymbol{e}}}_i = \dot{\boldsymbol{\sigma}}_i - \dot{\hat{\boldsymbol{\sigma}}}_i = (A_i - L_iC_i)\hat{\boldsymbol{e}}_i + E_i\tau_i. \tag{10}$$

With this formulation, providing that d_i or τ_i is bounded, the error $\lim_{t\to\infty}\hat{\boldsymbol{e}}_i(t)$ will also be bounded with a suitable choice of L_i stabilizing dynamics (10), see (Yang and Huang, 2009; Abadi et al., 2020). From the estimation achieved in (9), let us define the virtual input v_i as follow:

$$v_i = \dot{\sigma}_{i,r_i\,ref} + K_i \begin{bmatrix} \sigma_{i,1\,ref} - \hat{\sigma}_{i,1} \\ ... \\ \sigma_{i,r_i\,ref} - \hat{\sigma}_{i,r_i} \end{bmatrix} - \hat{\sigma}_{i,(r_i+1)} \ , \quad (11)$$

where $K_i = [k_{i,1}\ k_{i,2}\ ...\ k_{i,r_i}]$ is the control matrix of tuning parameters and $\sigma_{i,s\,ref} \triangleq z_{i\,ref}^{(s-1)}$ $(1 \leq s \leq r_i)$.

Proposition 2. With the virtual input proposed in (11), and a suitable choice of L_i and K_i, the tracking and estimation error can be stabilized in closed-loop.

Proof. First, we rewrite (11) as:

$$v_i = \dot{\sigma}_{i,r_i\,ref} + K_i\boldsymbol{e}_i + \tilde{K}_i\hat{\boldsymbol{e}}_i - \sigma_{i,(r_i+1)} \ , \quad (12)$$

where $\tilde{K}_i = [K_i\ 1]$, $e_{i,s} = \sigma_{i,s\,ref} - \sigma_{i,s}$, $(1 \leq s \leq r_i)$ and $\boldsymbol{e}_i = [e_{i,1}\ ...\ e_{i,r_i}]^\top$. For further use, consider the notations:

$$A_i^* = \begin{bmatrix} \mathbf{0}_{(r_i-1)\times 1} & \boldsymbol{I}_{(r_i-1)} \\ 0 & \mathbf{0}_{1\times(r_i-1)} \end{bmatrix}, B_i^* = \begin{bmatrix} \mathbf{0}_{(r_i-1)\times 1}^\top & 1 \end{bmatrix}^\top . \quad (13)$$

Hence, on one hand, we may rewrite the tracking error as:

$$\dot{\boldsymbol{e}}_i = \frac{d}{dt}\begin{bmatrix} \sigma_{i,1\,ref} - \sigma_{i,1} \\ \dots \\ \sigma_{i,r_i\,ref} - \sigma_{i,r_i} \end{bmatrix} = A_i^*\boldsymbol{e}_i + B_i^*\dot{\sigma}_{i,r_i\,ref} - B_i^*\dot{\sigma}_{i,r_i}. \quad (14)$$

On the other hand, applying the virtual input (12) to the dynamics in (1) and then replacing the value of $\dot{\sigma}_{i,r_i} = z_i^{(r_i)}$ into equation (14), we obtain the closed loop for the tracking error dynamics as:

$$\begin{aligned} \dot{\boldsymbol{e}}_i &= A_i^*\boldsymbol{e}_i + B_i^*\dot{\sigma}_{i,r_i\,ref} - B_i^*(\dot{\sigma}_{i,r_i\,ref} + K_i\boldsymbol{e}_i + \tilde{K}_i\hat{\boldsymbol{e}}_i) \\ &= (A_i^* - B_i^*K_i)\,\boldsymbol{e}_i - B_i^*\tilde{K}_i\hat{\boldsymbol{e}}_i. \end{aligned} \quad (15)$$

Rearranging (10) and (15), we have:

$$\frac{d}{dt}\begin{bmatrix} \boldsymbol{e}_i \\ \dot{\boldsymbol{e}}_i \end{bmatrix} = \begin{bmatrix} (A_i^* - B_i^*K_i) & -B_i^*\tilde{K}_i \\ \mathbf{0}_{(r_i+1)\times r_i} & (A_i - L_iC_i) \end{bmatrix}\begin{bmatrix} \boldsymbol{e}_i \\ \hat{\boldsymbol{e}}_i \end{bmatrix} + \begin{bmatrix} \mathbf{0}_{r_i\times 1} \\ E_i \end{bmatrix}\tau_i. \quad (16)$$

From here we clearly ensure the stability of the closed-loop with a right choice of the controller's and observer's poles (respectively in (15) and (10)) knowing that the observability for (6) and controllability for (13) are satisfied.

The evaluation of the system's performance is now also facilitated via the linearization. In the next subsection, we recall the construction of an approximation of the minimal robust positive invariant (mRPI) set, Stoican et al. (2015a). This is useful for confining the system's trajectory and quantifying its performance based on the chosen poles for the linear controllers.

2.3 Tight approximation for the mRPI set

While there exist various methods to construct RPI sets, the issue is still open (Blanchini and Miani, 2008). The computation time, the complexity of the result and even the fact that often the procedures are designed for the discrete-time case are significant hurdles. In this section we propose an extension of the result for the discrete-case from Stoican et al. (2015a) which in turn is based on the null-controllable set construction from Hu et al. (2002). We consider the autonomous LTI system:

$$\dot{\boldsymbol{\xi}}(t) = A\boldsymbol{\xi}(t) + \boldsymbol{d}\delta(t), \quad (17)$$

with $\boldsymbol{\xi}(t) \in \mathbb{R}^n$ the state vector, $\delta(t) \in [-1;\ 1]$ a scalar disturbance, $A \in \mathbb{R}^{n\times n}$ a stable state-matrix and $\boldsymbol{d} \in \mathbb{R}^n$. The key factors are: i) the stability of A (a reasonable assumption as long as (17) denotes a closed-loop dynamics); and, ii) the disturbance affecting the dynamics is given by a scalar (again reasonable, as this is the case in many applications where the disturbance is bounded element-wise). Without detailing the apparatus, we note that the construction is based on three interlocking elements:

i) a monotonously increasing sequence of $n-1$ moments

$$\mathbf{t} = \{t_1 \leq t_2 \leq \cdots \leq t_{n-1}\}; \quad (18)$$

ii) a vector $c_{\mathbf{t}} \in \mathbb{R}^d$ which verifies

$$c_{\mathbf{t}}^\top e^{At_i}\boldsymbol{d} = 0,\ \forall 1 \leq i \leq n-1; \quad (19)$$

iii) a sequence of extremal points

$$\boldsymbol{\xi}_{\mathbf{t}}^\star = \left(2\sum_{i=1}^{n-1}(-1)^i e^{At_i} + (-1)^n\boldsymbol{I}_n\right)A^{-1}\boldsymbol{d}. \quad (20)$$

Let Ω_∞ be the mRPI associated with (17). As detailed elsewhere (Stoican et al. (2015a)), extremal points (20) sit on the boundary of Ω_∞ and hyperplanes $\{\boldsymbol{\xi} \in \mathbb{R}^d : c_{\mathbf{t}}^\top\boldsymbol{\xi} = \pm c_{\mathbf{t}}^\top\boldsymbol{\xi}_{\mathbf{t}}^\star\}$ are support hyperplanes to Ω_∞, tangent to it at $\boldsymbol{\xi}_{\mathbf{t}}^\star$. Thus any finite sequence of points (20) provides an inner approximation (in generator form) while the corresponding sequence of normal vectors (19) provides an outer approximation (in half-space form) of Ω_∞:

$$\begin{aligned} \underline{\Omega}_{\mathbb{T}} = \left\{\boldsymbol{\xi} \in \mathbb{R}^n : \boldsymbol{\xi} = \sum_{\mathbf{t}\in\mathbb{T}} \alpha_{\mathbf{t}}^{\pm}\,(\pm\boldsymbol{\xi}_{\mathbf{t}}^\star)\,, \forall\alpha_{\mathbf{t}}^{\pm} \geq 0, \sum_{\mathbf{t}\in\mathbb{T}}\alpha_{\mathbf{t}}^{\pm} = 1\right\} \\ \subset \Omega_\infty \subset \overline{\Omega}_{\mathbb{T}} = \left\{\boldsymbol{\xi} \in \mathbb{R}^n :\ |c_{\mathbf{t}}^\top\boldsymbol{\xi}| \leq |c_{\mathbf{t}}^\top\boldsymbol{\xi}_{\mathbf{t}}^\star|,\ \forall\mathbf{t} \in \mathbb{T}\right\}, \end{aligned} \quad (21)$$

where $\mathbb{T}$ denotes a list of sequences as in (18).

Having both inner and outer approximations as in (21) allows to bracket Ω_∞ arbitrarily tight (without any iterative procedure!) and, equally important, to have an upper bound of the approximation error (e.g., the Hausdorff distance between $\underline{\Omega}_{\mathbb{T}}$ and $\overline{\Omega}_{\mathbb{T}}$). It is simpler, from an implementation viewpoint, to start with a collection of time-sequences $\mathbb{T} = \{\mathbf{t}\}$ from which to construct both $c_{\mathbf{t}}$ as in (19) and $\boldsymbol{\xi}_{\mathbf{t}}^\star$ as in (20). Two details are worthwhile of mentioning. First, note that (19) provides $n-1$ equalities for an $\mathbb{R}^n$ vector. To uniquely identify it, we add an n-th regularization equality, $c_{\mathbf{t}}^\top\mathbf{1} = 1$. Second, among the time sequences $\mathbf{t}$ we consider $\{0,\dots,0\}$ and $\{\infty,\dots,\infty\}$ as those correspond to the fix points of the dynamic for $\delta(t) = \pm 1$, i.e., the steady state values $\boldsymbol{\xi}_{\pm}^\star = \mp A^{-1}b$.

The above mRPI construction, (21) will be instrumental in the next sections for evaluating the controllers' and observers' performance.

3. CONTROL DESIGN FOR A FIXED-WING UAV

In this section, we implement the two design procedures for a 3-DOF UAV model. We will first use the optimal trajectory generation solution proposed in (Do et al., 2021) to set up the reference for the system. Then we provide two flat outputs which will be further used for analyzing the performance of the tracking controller design. Simulations, comparisons and discussions are addressed in Section 4.

3.1 3-DOF fixed-wing UAV model

Consider the fixed-wing model (Stoican et al., 2015b):

$$\begin{aligned} \dot{x} &= V_a\cos\psi + d_x, \\ \dot{y} &= V_a\sin\psi + d_y, \\ \dot{\psi} &= \frac{g\,\tan\phi}{V_a} + d_\psi, \end{aligned} \quad (22)$$

where x, y, ψ are the three states of the system denoting the positions and the heading angle of the UAV, respectively; $\boldsymbol{u} = [V_a,\ \phi]^\top$ denotes the two inputs of the system corresponding to the relative velocity and the bank angle.

Finally, d_x, d_y and d_ψ represent the bounded disturbances acting on the three states, their values will be considered zero when the nominal model is taken into account. The equations in (22) are rewritten in a form of (1) as:

$$\dot{\boldsymbol{\xi}} = f(\boldsymbol{\xi}, \boldsymbol{u}) + \boldsymbol{d}_\xi, \tag{23}$$

where $\boldsymbol{\xi} = [x, y, \psi]^\top$ and $\boldsymbol{d}_\xi = [d_x,\, d_y,\, d_\psi]^\top$.

3.2 Flat characterization of the UAV model

For the nominal model, there exist several flat outputs as shown in (Do et al., 2021), with the help of which, one may choose to compute the linearization law. In this application, we consider the following two flat output vectors for which we analyse the differences in performance with respect to disturbance rejection (see Sections 2.2 and 2.1). The first flat output we study is:

$$\boldsymbol{z}^1 = \begin{bmatrix} z_1^1 & z_2^1 \end{bmatrix}^\top \triangleq [x\ y]^\top, \tag{24}$$

while the second is:

$$\boldsymbol{z}^2 = \begin{bmatrix} z_1^2, & z_2^2 \end{bmatrix}^\top \triangleq \begin{bmatrix} \sqrt{x^2+y^2}, & \arctan(y/x) \end{bmatrix}^\top. \tag{25}$$

where the superscript denotes the currently considered flat output, its corresponding representation and parameters.

First flat representation: With the flat output given in (24), we express the inputs in the form of (2b) as follows:

$$\begin{cases} V_a &= \sqrt{(\dot{z}_1^1)^2 + (\dot{z}_2^1)^2}, \\ \tan\phi &= \dfrac{\ddot{z}_2^1 \dot{z}_1^1 - \ddot{z}_1^1 \dot{z}_2^1}{g\sqrt{(\dot{z}_1^1)^2 + (\dot{z}_2^1)^2}}. \end{cases} \tag{26}$$

To linearize the model, evidently, V_a requires a dynamical extension so that the relation between high order derivatives of the flat output and the extension is invertible. Specifically, introduce the augmented state $\eta = V_a$ and $u_\eta = \dot{\eta}$ into the nominal model of (22):

$$\begin{aligned} \dot{x} &= \eta\cos\psi, \quad \dot{\psi} = \frac{g\,\tan\phi}{\eta}, \\ \dot{y} &= \eta\sin\psi, \quad \dot{\eta} = u_\eta, \end{aligned} \tag{27}$$

then the inputs $[u_\eta,\, \tan\phi]$ of the new system yields:

$$\begin{aligned} u_\eta &= \frac{\dddot{z}_1^1 \dot{z}_1^1 + \ddot{z}_2^1 \dot{z}_2^1}{\sqrt{(\dot{z}_1^1)^2 + (\dot{z}_2^1)^2}} \\ \tan\phi &= \frac{\ddot{z}_2^1 \dot{z}_1^1 - \ddot{z}_1^1 \dot{z}_2^1}{g\sqrt{(\dot{z}_1^1)^2 + (\dot{z}_2^1)^2}}. \end{aligned} \tag{28}$$

Subsequently, the dynamics are linearized by replacing $\ddot{z}_1^1, \ddot{z}_2^1$ respectively by the virtual input v_1^1, v_2^1 into (28) which , when introduced in (22), leads to:

$$\ddot{z}_i^1 = v_i^1 + d_i^1, \ \ (i \in \{1,2\}) \tag{29}$$

where d_1^1 and d_2^1 are the propagated disturbances affecting the flat output which are assumed to be bounded and, through linearization (28), are shown to be:

$$\begin{aligned} d_1^1 &= \dot{d}_x - V_a d_\psi \sin\psi, \\ d_2^1 &= \dot{d}_y + V_a d_\psi \cos\psi, \end{aligned} \tag{30}$$

where all states and control $\boldsymbol{u}$ have to be expressed in terms of the flat output like in (2), see (Do et al., 2021).

Second flat representation: The similar design procedure is applied for the second flat output, given in (25). With the same extension $\eta = V_a$, replacing $\ddot{z}_1^1, \ddot{z}_2^1$ respectively by the virtual input v_1^2, v_2^2 into the representation of the input $[u_\eta, \tan\phi]$ we define the linearizing control law as:

$$\begin{aligned} u_\eta &= \frac{v_2^2 \dot{z}_2^2 (z_1^2)^2 + v_1^2 \dot{z}_1^2 + (\dot{z}_2^2)^2 \dot{z}_1^2 z_1^2}{\sqrt{(\dot{z}_1^2)^2 + (z_1^2 \dot{z}_2^2)^2}}, \\ \tan\phi &= \frac{v_2^2 \dot{z}_1^2 z_1^2 - v_1^2 \dot{z}_2^2 z_1^2 + 2(\dot{z}_1^2)^2 \dot{z}_2^2 + (\dot{z}_2^2)^3 (z_1^2)^2}{g\sqrt{(\dot{z}_1^2)^2 + (z_1^2 \dot{z}_2^2)^2}}. \end{aligned} \tag{31}$$

Equation (31) then turns dynamics (22) into:

$$\ddot{z}_i^2 = v_i^2 + d_i^2, \ \ (i \in \{1,2\}) \tag{32}$$

where the propagation of the disturbance is expressed as:

$$\begin{aligned} d_1^2 = {} & \frac{x(\dot{d}_x - V_a d_\psi \sin\psi) + y(\dot{d}_y + V_a d_\psi \cos\psi)}{\sqrt{x^2+y^2}} \\ & + \frac{2V_a(d_x\cos\psi + d_y\sin\psi) + d_x^2 + d_y^2}{\sqrt{x^2+y^2}} \\ & + \frac{(x d_x + y d_y)(x d_x + y d_y + 2V_a(x\cos\psi + y\sin\psi))}{(\sqrt{x^2+y^2})^{3/2}} \\ d_2^2 = {} & \frac{x(\dot{d}_y - V_a d_\psi \cos\psi) + y(-\dot{d}_x + V_a d_\psi \sin\psi)}{x^2+y^2}. \end{aligned} \tag{33}$$

3.3 Tracking control design

In this subsection, the application of the procedure introduced in Section 2.2 is implemented for the UAV using the two linearized dynamics from (29) and (32). Since both of them share a common double-integrator form:

$$\ddot{z}_i^j = v_i^j + d_i^j \quad (\text{with } i,j \in \{1,2\}), \tag{34}$$

following Section 2.2, (34) is rewritten as:

$$\dot{\boldsymbol{\sigma}}_i^j = A_i^j\, \boldsymbol{\sigma}_i^j + B_i^j\, v_i^j + E_i^j\, \tau_i^j, \tag{35}$$

where the matrices are defined as:

$$\boldsymbol{\sigma}_i^j = [\sigma_{i,1}^j \quad \sigma_{i,2}^j \quad \sigma_{i,3}^j]^\top \triangleq [z_i^j \quad \dot{z}_i^j \quad d_i^j]^\top, \tag{36}$$

$$A_i^j = \begin{bmatrix} 0 & 1 & 0 \\ 0 & 0 & 1 \\ 0 & 0 & 0 \end{bmatrix}; B_i^j = \begin{bmatrix} 0 \\ 1 \\ 0 \end{bmatrix}; E_i^j = \begin{bmatrix} 0 \\ 0 \\ 1 \end{bmatrix}; \tau_i^j = \dot{d}_i^j. \tag{37}$$

Next, the observer is formulated similarly to (9) as:

$$\dot{\hat{\boldsymbol{\sigma}}}_i^j = A_i^j \hat{\boldsymbol{\sigma}}_i^j + B_i^j v_i^j + L_i^j (y_i^j - \hat{y}_i^j) \tag{38}$$

where $L_i^j \in \mathbb{R}^{3\times 1}$ is the tuning parameter for the estimator and $y_i^j = \sigma_{i,1}^j$ is the measured output. Equivalently, y_i^j may be rewritten as: $y_i^j = C_i^j\, \boldsymbol{\sigma}_i^j$ with $C_i^j = [1\ \ 0\ \ 0]$. The estimation error yields:

$$\dot{\hat{\boldsymbol{e}}}_i^j = \dot{\boldsymbol{\sigma}}_i^j - \dot{\hat{\boldsymbol{\sigma}}}_i^j = (A_i^j - L_i^j\, C_i^j)\, \hat{\boldsymbol{e}}_i^j + E_i^j \tau_i^j. \tag{39}$$

Using form (11), the virtual inputs v_i^j are constructed as:

$$v_i^j = \dot{\sigma}_{i,2\,ref}^j + K_i^j\, \boldsymbol{e}_i^j - \hat{\sigma}_{i,3}^j \tag{40}$$

where $\boldsymbol{e}_i^j = [e_{i,1}^j\ e_{i,2}^j]^\top \triangleq \begin{bmatrix} \sigma_{i,1\,ref}^j - \hat{\sigma}_{i,1}^j, & \sigma_{i,2\,ref}^j - \hat{\sigma}_{i,2}^j \end{bmatrix}^\top$ and $K_i^j \triangleq [k_{i,1}^j \quad k_{i,2}^j] \in \mathbb{R}^2$ denote the tracking error and the controller's gain respectively; the subscript "ref" implies the corresponding reference signal that the system needs to track i.e, $\sigma_{i,1\,ref}^j = z_{i\,ref}^j$ and $\sigma_{i2\,ref}^j = \dot{z}_{i\,ref}^j$. Finally, in accordance with Proposition 2, the closed-loop dynamics are written as:

$$\frac{d}{dt}\begin{bmatrix} \boldsymbol{e}_i^j \\ \hat{\boldsymbol{e}}_i^j \end{bmatrix} = \begin{bmatrix} A_i^{j*} - B_i^{j*} K_i^j & -B_i^{j*}\, \tilde{K}_i^j \\ \mathbf{0}_{3\times 2} & A_i^j - L_i^j C_i^j \end{bmatrix} \begin{bmatrix} \boldsymbol{e}_i^j \\ \hat{\boldsymbol{e}}_i^j \end{bmatrix} + \begin{bmatrix} \mathbf{0}_{2\times 1} \\ E_i^j \end{bmatrix} \tau_i^j, \tag{41}$$

with $A_i^{j*} = \begin{bmatrix} 0 & 1 \\ 0 & 0 \end{bmatrix}$; $B_i^{j*} = \begin{bmatrix} 0 \\ 1 \end{bmatrix}$; $\tilde{K}_i^j = [K_i^j \quad 1]$. Then by a suitable choice of poles for dynamics (41), with the help of K_i^j and L_i^j, we can ensure its stability under the effect of the disturbance τ_i^j. Finally, since system (41) is under form (17), we can compute the approximation of the mRPI set given in (21), for each pair of $(i,j) \in \{1,2\}^2$, denoted respectively by Ω_i^j.

4. SIMULATION RESULTS

4.1 Numerical simulation

For illustration purposes, numerical simulation will be carried out in this section. For all $i, j \in \{1,2\}$ the

poles of the closed-loop system, given by (41) will be placed identically. Furthermore, it is also assumed that the bounds of τ_i^j are numerically computed via their representations in (30), (33) and simulations. Simulation specifications are given in Table 1.

Table 1. Simulation specifications

Variables	Values
$[x(0),\, y(0),\, \psi(0)]^\top$	$[54 \quad 160 \quad 1.8726]^\top$
w_x	$0.5\sin(0.2t)$
w_y	$-0.2\cos(0.5t)$
w_ψ	$-0.05\sin(0.5t)$
V_a	$10 \leq V_a \leq 30$
$\tan\phi$	$-0.6 \leq \tan\phi \leq 0.6$
K_i^j	$[12 \quad 7]$
L_i^j	$[15.5 \quad 59.5 \quad 45]^\top$

For defining the reference signal, let us briefly recall the optimal trajectory framework in (Stoican et al., 2015b) with the way-point passing constraints described by:

$$\mathbb{W} = 10^2 \times \left\{ \begin{bmatrix}0.5\\1.6\end{bmatrix}, \begin{bmatrix}0.7\\2.5\end{bmatrix}, \begin{bmatrix}1.9\\2.7\end{bmatrix}, \begin{bmatrix}2.8\\1.6\end{bmatrix}, \begin{bmatrix}3.6\\0.6\end{bmatrix}, \begin{bmatrix}5\\1.75\end{bmatrix} \right\} \quad [m]$$

$$\mathbb{T}_W = \{0, 8, 16, 24, 32, 40\} \;\; [s], \tag{42}$$

where $\mathbb{W}$ is the set of way-points that the system needs to pass through at the associated time stamps in $\mathbb{T}_W$. The trajectory here is parametrized as a weighted sum of 7 B-spline functions or order 5 (which ensures passing through the way-points of (42) and guarantees curve smoothness for up to its 4th order derivative).

With the reference represented by the dashed red curve, Fig. 2 depicts the tracking performances of the two controllers deduced from the two flat outputs (respectively denoted by Ctrl. 1 and Ctrl. 2). Simultaneously, by calculating the outer approximation of the mRPI set, given in (21), of (41) for each pair of $i, j \in \{1, 2\}$, we obtain two pairs of polytopic sets corresponding to the two flat representations. The projections of each pair into Cartesian coordinates are also depicted in Fig. 2 with the notation of $\overline{\Omega}_j$ which corresponds to the controller Ctrl. j.

We provide also different scenarios in Table 2 for which the poles of the closed loop are chosen differently. Let p_c and p_o denote the poles for the controllers and observers respectively. $RMS(e_{lj})$, with $l \in \{x, y\}$ and $j \in \{1, 2\}$, represents the root mean square (RMS) of the tracking error on the l axis implemented with the Ctrl. j. Finally, let us consider the perturbation in the form of $[d_x, d_y, d_\psi]^\top = [0.5\sin\omega t, -0.2\cos\omega t, -0.05\sin\omega t]^\top$ to analyse the system response under different frequencies ω of the perturbation. Illustrations of the RMS of the tracking error are provided in Fig. 3.

4.2 Discussions

In the following we address some remarks on the approach implemented over the UAV model and the analysis of different effects on the system's performance led by the change in the flat outputs.

Control design: As a powerful combination, flatness and ESO provide a framework for not only estimating the states' value but also rejecting the disturbances in nonlinear control design. However, although the system's error may be proven to be bounded, this confirmation can only be drawn after the choice of the poles in the observer and the controller designs. This yields the question if there exist more efficient choices for the gains K_i^j and L_i^j in the sense that there will be less energy spent on the input while the tolerance for the error is still satisfied. Besides, from the frequency domain standpoint, in order to filter out the perturbation, the poles must be chosen differently due to the variation (in amplitude, in frequency) of the original disturbance via the linearization procedure. Likewise, it is noted in Fig. 3 that for the same choice of poles, the errors' RMS behave differently in the frequency domain. Hence, this issue needs to be studied at the parameters' tuning stage. Moreover, (30) and (33) have different dependence on the derivative degree of the original disturbance, posing the need to consider the smoothness of disturbances while choosing among the representations.

Analysis for different flat outputs: As aforementioned, the bounded or stable tracking error of flat outputs provides insights on the system's tracking errors. Particularly, as seen in the simulations for the UAV model, the two trajectories resulting from the two different controllers lie within the tubes computed from two different flat representations (Fig. 2). However, it is notable that the geometrical size and orientation of the tubes' cross-section vary along its trajectory. This comes from the fact that these two flat outputs do not have the same physical interpretation. Specifically, from a geometrical viewpoint, the first flat output represents the Cartesian position of the UAV while the second one corresponds to the UAV's distance from the origin and the angular coordinate in cylindrical coordinates. Therefore, when plotted in Cartesian coordinates, the tube from the second flat representation changes its volume depending on the UAV's position.

Moreover, as discussed previously, the choice of flat output directly affects the propagated disturbances acting on the virtual input, which may suggest that, the storage and processing requirements of a particular flat representation should not be neglected. Moreover, as stated in Table 2, the first control law performs better compared to the second one in all scenarios, implying that in this context, the best choice with respect to tracking performance may be the first controller. However, analytical proofs are still definitely required to certify this observation.

Furthermore, it should be also noted that these two flat representations allow us to represent the sets in the original coordinates, facilitating the comparison between their performance. However, with more complicated flat outputs, e.g., as the ones mentioned in (Do et al., 2021), the comparison is no longer evident (or applicable at all).

Finally, the specific choice of the flat output influences the disturbance and thus, the shape and size of the invariant sets associated to the tracking and estimation errors. This becomes especially relevant in the case of complex dynamics and/or strongly nonlinear flat representations.

5. CONCLUSION

This paper presented the procedure of disturbance rejection via extended observers in the context of trajectory generation and tracking of nonlinear differentially flat systems. Furthermore, an insightful analysis was carried out related to the difference in the tracking performance while using various flat representations. Simulations results and comparisons for a fixed-wing aerial vehicle suggested not only certain future directions for further improvement, but

Table 2. Tracking performance with different controller and observer poles

p_c	p_o	RMS(e_{x1})	RMS(e_{y1})	RMS(e_{x2})	RMS(e_{y2})
$[-2;-1.5]$	$[-10;-4.5;-1]$	0.67	0.41	3.98	4.11
$[-4;-3]$	$[-10;-4.5;-1]$	0.47	0.14	1.10	1.03
$[-4;-3]$	$[-10;-6;-3]$	0.49	0.16	1.11	1.04

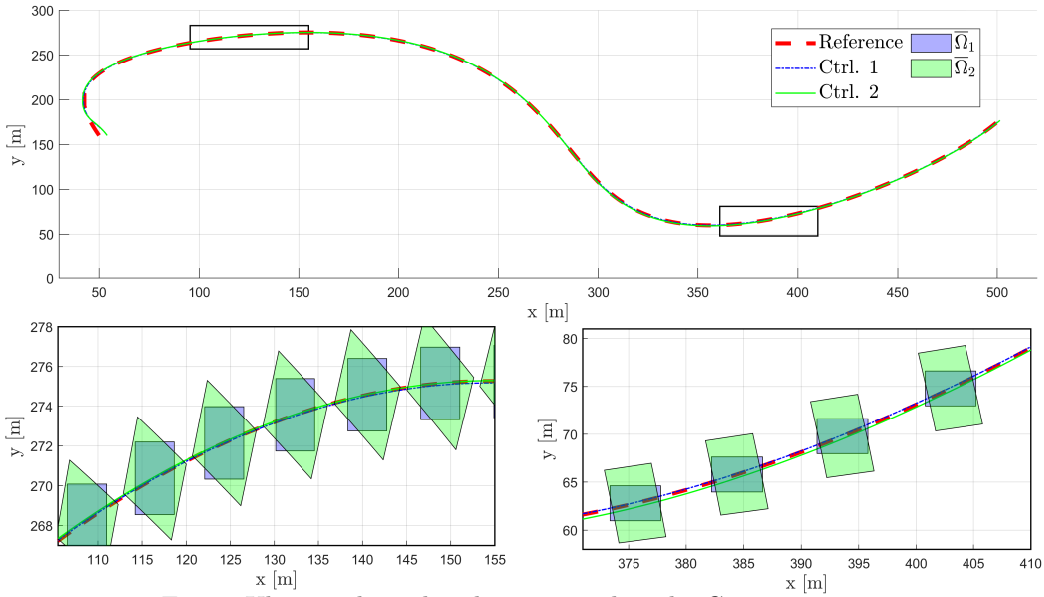

Fig. 2. Ultimate bounds tube projected in the Cartesian space.

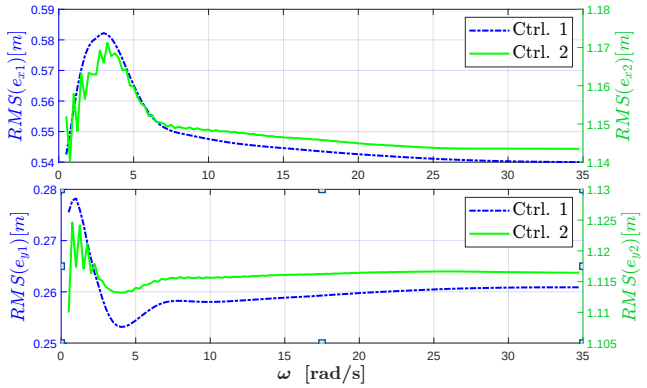

Fig. 3. RMS of tracking errors under disturbances with different frequencies.

also what kind of phenomena and difficulties one may face when considering more complex systems.

REFERENCES

Abadi, A., El Amraoui, A., Mekki, H., and Ramdani, N. (2020). Robust tracking control of quadrotor based on flatness and active disturbance rejection control. *IET Control Theory & Applications*, 14(8), 1057–1068.

Blanchini, F. and Miani, S. (2008). *Set-theoretic methods in control*. Springer.

Do, H.T., Prodan, I., and Stoican, F. (2021). Analysis of alternative flat representations of a UAV for trajectory generation and tracking. In *2021 25th International Conference on System Theory, Control and Computing (ICSTCC)*, 58–63. IEEE.

Fliess, M., Lévine, J., Martin, P., and Rouchon, P. (1993). On differentially flat nonlinear systems. In *Nonlinear Control Systems Design 1992*, 159–163. Elsevier.

Hu, T., Lin, Z., and Qiu, L. (2002). An explicit description of null controllable regions of linear systems with saturating actuators. *Systems & control letters*, 47(1), 65–78.

Kaminski, Y.J., Lévine, J., and Ollivier, F. (2018). Intrinsic and apparent singularities in differentially flat systems, and application to global motion planning. *Systems & Control Letters*, 113, 117–124.

Levine, J. (2009). *Analysis and control of nonlinear systems: A flatness-based approach*. Springer Science & Business Media.

Martin, P. (1994). Endogenous feedbacks and equivalence; systems and networks: Mathematical theory and applications. *Proc. MTNS'93*, 2, 343–346.

Nguyen, N.T., Prodan, I., and Lefèvre, L. (2020). Flat trajectory design and tracking with saturation guarantees: a nano-drone application. *International Journal of Control*, 93(6), 1266–1279.

Sira-Ramírez, H. (2015). Differential flatness and sliding mode control. In *Sliding Mode Control*, 211–252. Springer.

Stoican, F., Oară, C., and Hovd, M. (2015a). RPI approximations of the mRPI set characterizing linear dynamics with zonotopic disturbances. In *Developments in Model-Based Optimization and Control*, 361–377. Springer.

Stoican, F., Prodan, I., and Popescu, D. (2015b). Flat trajectory generation for way-points relaxations and obstacle avoidance. In *2015 23rd Mediterranean Conference on Control and Automation (MED)*, 695–700. IEEE.

Yang, X. and Huang, Y. (2009). Capabilities of extended state observer for estimating uncertainties. In *2009 American Control Conference*, 3700–3705. IEEE.

Zafeiratou, I., Prodan, I., Lefèvre, L., and Piétrac, L. (2020). Meshed DC microgrid hierarchical control: A differential flatness approach. *Electric Power Systems Research*, 180, 106133.